IOSUD – UNIVERSITATEA „DUNĂREA DE JOS”
DIN GALAȚI

Doctoral School of Fundamental and Engineering Sciences

SUMMARY
PhD THESIS

MULTIFUNCTIONAL HYBRID MATERIALS BASED ON SYNTHETIC AND NATURAL POLYMERS

PhD student,
Ing. Viorica (GHISMAN) PLEȘCAN

Scientific leader,
Prof.dr.chim. Viorica MUȘAT

Seria I 5: Ingineria Materialelor Nr. 13

GALAȚI

2019

IOSUD – UNIVERSITATEA „DUNĂREA DE JOS”
DIN GALAȚI

Doctoral School of Fundamental and Engineering Sciences

SUMMARY
PhD THESIS

MULTIFUNCTIONAL HYBRID MATERIALS BASED ON SYNTHETIC AND NATURAL POLYMERS

PhD student
Ing. Viorica (GHISMAN) PLEȘCAN

President, Prof univ.dr.ing. Gabriela-Elena BAHRIM
Scientific leader, Prof univ.dr.chim. Viorica MUȘAT
Scientific references, CS I dr. chim. Oana CARP
CS I dr. ing. Roxana Mioara PITICESCU
Prof univ.dr.chim. Rodica Mihaela DINICĂ

Seria I 5: Ingineria Materialelor Nr. 13
GALAȚI
2019

Seriile tezelor de doctorat susținute public în UDJG începând cu 1 octombrie 2013 sunt:

Domeniul fundamental ȘTIINȚE INGINEREȘTI

Seria I 1**:** **Biotehnologii**
Seria I 2**:** **Calculatoare și tehnologia informației**
Seria I 3: **Inginerie electrică**
Seria I 4**:** **Inginerie industrială**
Seria I 5: **Ingineria materialelor**
Seria I 6**:** **Inginerie mecanică**
Seria I 7**:** **Ingineria produselor alimentare**
Seria I 8: **Ingineria sistemelor**
Seria I 9**:** **Inginerie și management în agicultură și dezvoltare rurală**

Domeniul fundamental ȘTIINȚE SOCIALE

Seria E 1: **Economie**
Seria E 2: **Management**
Seria SSEF: **Știința sportului și educației fizice**

Domeniul fundamental ȘTIINȚE UMANISTE ȘI ARTE

Seria U 1: **Filologie- Engleză**
Seria U 2: **Filologie- Română**
Seria U 3**:** **Istorie**
Seria U 4: **Filologie - Franceză**

Domeniul fundamental MATEMATICĂ ȘI ȘTIINȚE ALE NATURII

Seria C: **Chimie**

Domeniul fundamental ȘTIINȚE BIOLOGICE ȘI BIOMEDICALE

Seria M: **Medicină**

TABLE OF CONTENTS

INTRODUCTION

An important part of the recent studies is focused on the development of new high performance biocompatible hybrid polymeric materials, using nanotechnology. Materials based on biocompatible and/or biodegradable polymers offer a fascinating field of interdisciplinary research on the frontier between materials science, nanotechnology and biotechnology.

An increased interest in the field of materials science and engineering presents the synergistic combination of the characteristics and performances of some inorganic compounds with the specific properties of an organic compound in order to develop hybrid materials having new properties and functions.

Hybrid materials based on metal oxide nanoparticles dispersed in organic polymers have been intensively studied in recent years due to the fact that they are new materials with special properties, resulting from the direct binding, at the molecular level, of the organic and inorganic components. Inorganic components at the nanometric dimensions can have optical and electrical properties, while polymers can bring advantages such as stabilization and control of the size and dispersibility of metal oxide nanoparticles.

Regarding electronic applications, the emergence of organic and flexible electronics has encouraged the search for new semiconductor and dielectric organic materials,

especially organic hybrid materials for applications in devices such as solar cells and thin film transistors.

Natural polysaccharide compounds represent an important group of compounds essential for the development of vital processes in living organisms, which have important biological and chemical properties such as: biocompatibility, biodegradability, polyfunctionality, sorption and chelatization capacity, high chemical reactivity. Starting from the structure of these compounds, through controlled chemical modifications, multifunctional macromolecular structures such as gels and hydrogels, polymeric resins, membranes, fibers and composites with applications in various fields of activity were obtained.

This work addresses the synthesis by chemical methods from the solution of two groups (films and profiled materials) of multifunctional hybrid materials based on oxide nanoparticles (ZrO_2, ZnO and Ag:ZnO) embedded in complex matrices of bioactive natural polymers (chitosan) and biocompatible synthetic polymers (PMMA), as well as biomimetic synthesis of chitosan-hydroxyapatite hybrid coatings.

The experimental researches presented in the paper were initiated and carried out within the Center of Nanostructures and Multifunctional Materials-CNMF / Laboratory of Chemical Nanotechnologies at the Faculty of Engineering, "Dunărea de Jos" University of Galați. Part of the studies on hybrid thin films based on nanoparticles-CS-

PMMA was carried out at the CENIMAT / I3N Research Center (Center of Materials Investigation - Institute of Nanostructures, Nanomodelling and Nanofabrication) at the NOVA University of Lisbon, on the occasion external mobility through the ERASMUS + Program (May-July 2017). The research on the synthesis of functional hybrid materials for prosthetics was carried out in collaboration with the Faculty of Dental Medicine at the OVIDIUS University of Constanța. Part of the characterization of these materials was carried out in collaboration with the ”Ilie Murgulescu” Institute of Physical Chemistry in Bucharest.

In completing the thesis, I also benefited from the financial support of the PN-II-PT-PCCA Project, Contract No.27 / 2014-NANOZON and the ERASMUS + Program (external mobility at CENIMAT/FCT/UNL 2017).

The general objective of the research presented in the paper consisted in obtaining new hybrid materials based on natural polymers (CS) and oxide nanoparticles embedded in polymeric matrix for various fields of applications, in the form of hybrid dielectric films for applications in transparent electronics and/or flexible, which may also have antimicrobial properties suitable for use in the biomedical field, but also multifunctional materials or coatings for prosthetics.

The specific objectives were:

- Obtaining of dielectric hybrid films by chemical solution methods and advanced characterization of films obtained

on the basis of oxide nanoparticles (ZrO_2, ZnO and Ag:ZnO) embedded in chitosan and PMMA.

- Obtaining hybrid materials based on oxide nanoparticles (ZnO and Ag: ZnO) embedded in chitosan and acrylic matrix and characterizing them for use as dental prostheses with antimicrobial properties.

- Obtaining increased biomimetic hybrid layers of chitosan-hydroxyapatite on demineralized tooth enamel substrate and characterizing them for their use as synthetic protective coatings.

The thesis is structured in seven chapters as follows:

Chap. 1, entitled "**The current state of production and applications of multifunctional hybrid materials based on natural compounds and acrylic polymers**", presents current state in the data in the literature on obtaining multifunctional hybrid materials based on synthetic acrylic polymers and natural polymers (polysaccharides and apatites), as well as their composites with oxide nanoparticles. Applications of these materials in transparent electronics and in the biomedical field are also discussed.

Chap. 2, entitled "**Research Methodology**", presents the experimental details on obtaining thin films and materials based on oxide nanoparticles (ZrO_2, ZnO and Ag:ZnO) embedded in chitosan and PMMA matrix, as well as on chitosan-hydroxyapatite biomimetic hybrid layers. The equipment and techniques used for the morphological,

structural, thermal, optical, electrical and functional characterization of the obtained multifunctional hybrid materials are presented.

Chap. 3, entitled "**Contributions to the preparation of thin films based on oxide nanoparticles embedded in chitosan and PMMA**", presents experimental results on morphology, chemical structure, thermal stability, optical properties and electrical behavior of thin films based on oxide nanoparticles (ZrO_2, ZnO and Ag:ZnO) in chitosan and PMMA.

Chap. 4, entitled "**Contributions to the obtaining of the hybrid materials based on chitosan in acrylic matrix** ", presents experimental results on obtaining two series of hybrid materials by mixing the commercial acrylic matrix Duracryl Plus with chitosan solution. The effect of the concentration and the order of the addition of chitosan solution in the acrylic matrix on the morphology, structure and thermal properties of the obtained hybrid materials are analyzed.

Chap. 5, entitled "**Contributions to obtaining hybrid materials based on oxide nanoparticles embedded in chitosan and acrylic matrix**", presents experimental results on obtaining four series of hybrid materials by mixing the commercial acrylic matrix Duracryl Plus with ZnO and Ag:ZnO nanoparticles and ZnO/CS and Ag:ZnO/CS composite nanoparticles. The effect of concentration and different types of oxide and composite

nanoparticles in acrylic matrix on the morphology, structure and thermal and antimicrobial properties of the obtained hybrid materials were analyzed.

Chap. 6, entitled "**Contributions to obtaining chitosan-HAP biomimetic hybrid coatings**", presents experimental results on obtaining two series of hybrid coatings by biomimetic growth of hydroxyapatite in the presence of the commercial Emdogain hydrogel (first series) and an chitosan-Emdogain based hydrogel (second series). The effect of the hydrogel used and the growth time of the biomimetic layers in artificial saliva on the morphology, structure and mechanical properties are analyzed.

Chap. 7, contains "**Final conclusions and personal contributions**" resulting from the research presented in this paper. Also the published articles and the participation in national and international conferences, as well as the **future research directions** expected to be developed based on the results obtained in the presented study. The paper contains a list of notations and abbreviations, the list of figures and the list of tables regarding the scientific data presented in chapters 1-6 and the list of bibliographic references used in the study presented in the paper.

The novelty and originality elements of the thesis are:

- Obtaining dielectric hybrid thin films based on oxides (ZrO_2, ZnO and Ag:ZnO) and polymers (chitosan and PMMA), with high capacitance values (maximum 1200 nF) at temperatures below 200 °C.

Hybrid films with complex compositions similar to those presented in this paper have not been reported in the literature.

- Modification of Duracryl Plus commercial materials with complex hybrid nanoparticles (ZnO/CS and Ag:ZnO/CS) with improved biocompatible and antimicrobial properties to obtain new multifunctional hybrid materials with applications in prosthetics.
- Obtaining hybrid chitosan-HAP biomimetic layers with a structure similar to natural enamel.

CHAPTER 1

CURRENT STATUS ON OBTAINING AND APPLICATIONS OF MULTIFUNCTIONAL HYBRID MATERIALS BASED ON NATURAL COMPOUNDS AND ACRYLIC POLYMERS

This chapter presents the current state of obtaining of multifunctional hybrid materials based on acrylic synthetic polymers, natural polysaccharide and phosphate-calcium polymers and their composites with oxide nanoparticles. Applications of these materials in transparent electronics and biomedical fields are also discussed.

1.1 Complex materials based on synthetic and natural biocompatible polymers

Synthetic and natural polymeric materials represent a very important class of raw materials for obtaining biocompatible and bioactive materials designed to meet specific requirements for applications in transparent and flexible electronics and in biomedical fields. Their selection is made according to the key features of the "device" such as solubility, permeability, degradability, transparency and mechanical strength, but the polymers currently available must be improved by changing the surface properties. Therefore, the design of macromolecules must be carefully adapted to ensure the combination of the chemical,

biological and mechanical functions required for the manufacture of new multifunctional biomaterials [1].

The combination of polymers has become a solution for providing polymeric materials with new properties suitable for practical applications.

Hybrid materials based on metal oxide nanoparticles dispersed in organic polymers have been intensively studied in recent years due to the fact that they are new materials with special properties.

1.2.1 Types of interactions in hybrid materials

The term hybrid material is used for many different systems that span a wide range of different materials, such as highly ordered crystalline coordination polymers, amorphous sol-gel compounds, materials with and without interactions between inorganic and organic components [79] .Organic-inorganic hybrid materials can be defined as multicomponent compounds having at least one organic and one inorganic component in the field of submicron or nanometric dimensions [80]. The properties of hybrid materials do not represent a simple summation of the properties of the individual components, but a synergistic cumulation of them, created by the presence of a very large surface hybrid interface [81].

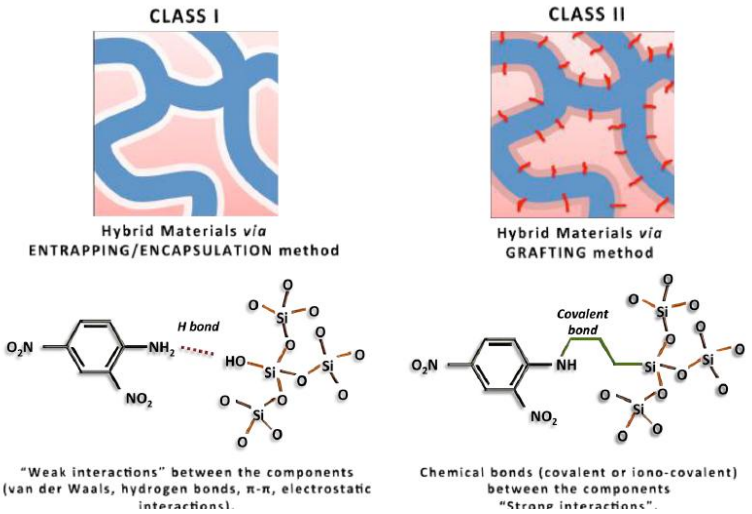

Fig. 1.14 Classification of hybrid materials according to the type of interactions ("weak" or "strong") and the related structure [82]

The organic-inorganic interface plays a major role in adjusting the properties of chemical and thermal, catalytic, optical, mechanical stability. The hybrid materials were classified into two main families, depending on the nature of the interface between the organic (or biological) component and the mineral component (Fig. 1.14). So:

- **Class I** includes hybrid systems in which organic and inorganic components interact through weak Van der Waals, hydrogen or electrostatic bonds.

- **Class II** corresponds to hybrid materials in which the organic and inorganic components are linked by

stronger chemical bonds of covalent or ionic-covalent type [83].

Fig. 1.15 Commercial applications of hybrid materials in all areas [83]

The number of applications that refer to hybrid nanomaterials has grown steadily over the last 20 years and the field is expanding. Some of the most important fields of industrial applications of hybrid nanomaterials are shown in Fig. 1.15.

CHAPTER 2

RESEARCH METHODOLOGY

This chapter presents the experimental details on obtaining complex hybrid materials based on oxide nanoparticles (ZrO_2, ZnO and Ag: ZnO) incorporated in PMMA or PMMA-chitosan matrices, in the form of thin dielectric films and in the form of composite materials for prosthetics. . Hybrid layers based on natural biopolymers, chitosan (CS) and hydroxyapatite (HAP), were grown biomimically on demineralized natural enamel.
Also presented are the methods, techniques and equipment used for morphological, structural, thermal, optical, electrical and mechanical characterization (in the case of prosthetic materials) of the obtained multifunctional hybrid materials.

2.1.1 Hybrid thin films based on oxide nanoparticles embedded in chitosan and PMMA

This study aimed to incorporate the nanoparticles of ZrO_2, ZnO and Ag:ZnO into chitosan and PMMA arrays and to deposit them as thin films. The thin films were deposited using the sol-gel method, the spin-coating technique, and the parameter that varied was the number of layers. The films deposited were heat treated and the polymerization was carried out in the presence of UV radiation.

2.1.2 Hybrid materials based on chitosan in acrylic matrix

Two series of hybrid materials were obtained in which chitosan was added in different proportions and in different mixing modes with the acrylic components P and L: addition of CS before mixing P and L (series I) and after mixing them (series II)).

2.1.3 Hybrid materials based on oxide nanoparticles embedded in chitosan and acrylic matrix

The hybrid materials obtained by modifying the Duracryl Plus acrylic resin with different nanoparticle concentrations of ZnO, Ag:ZnO, ZnO/CS and Ag:ZnO/CS for prosthetics are shown in Fig. 2.1.

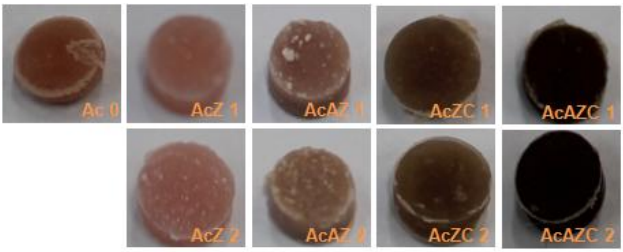

Fig. 2.1 Photo images of the hybrid materials obtained

2.1.4 Biomimetic increases of chitosan-HAP based hybrid biomaterials

HAP and HAP-CS layers were obtained by biomimetic growth in artificial saliva in the presence of EMD and EMD-

CS hydrogel respectively. The steps of obtaining the hybrid layers are shown in Fig. 2.2.

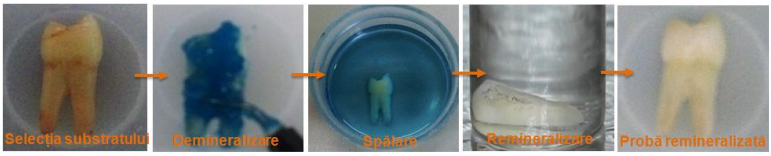

Fig. 2.2 The steps of obtaining by means of biomimetic growth of the HAP-CS hybrid layers on the artificial demineralized natural tooth enamel

2.4 Functional characterization of obtained hybrid materials

2.4.2 Measurement of electrical properties

For the electrical characterization of the obtained thin films, a Metal-Insulator-Semiconductor (MIS) structure was created (Fig. 2.4) in which the obtained dielectric film was placed between thin aluminum films, deposited by the physical vapor phase (PVD) method.), with a thickness of 80 nm, and the top electrodes were deposited using a mask with different diameters.

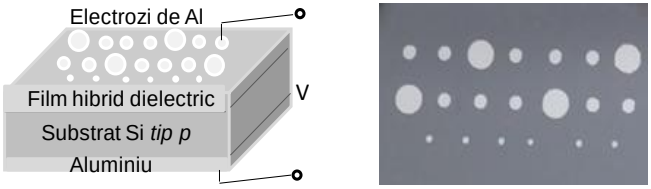

Fig. 2.4 Schematic representation of the Metal-Isolator-Semiconductor structure (a) and photo image on the surface of this MIS structure (b)

CHAPTER 3
CONTRIBUTIONS TO THE PREPARATION OF THIN FILMS BASED ON OXIDE NANOPARTICLES EMBEDDED IN CHITOSAN AND PMMA

This chapter presents the experimental results regarding the morphological, structural, thermal, optical, and electrical characterization of hybrid thin films based on oxide nanoparticles embedded in mixed chitosan (CS) and polymethylmethacrylate (PMMA) matrices.
The nanoparticles of ZrO_2, ZnO and Ag:ZnO were embedded in chitosan and PMMA and were deposited as thin films by the sol-gel method, spin coating technique. The influence of the number of layers for all three obtained systems was followed.

3.1 Thin films based on ZrO_2NPs-CS-PMMA

3.1.1 Chemical structure of precursors

Figure 3.1 shows the FTIR spectra of the precursors used and the hybrid soil obtained ZrO_2NPs-CS-PMMA.

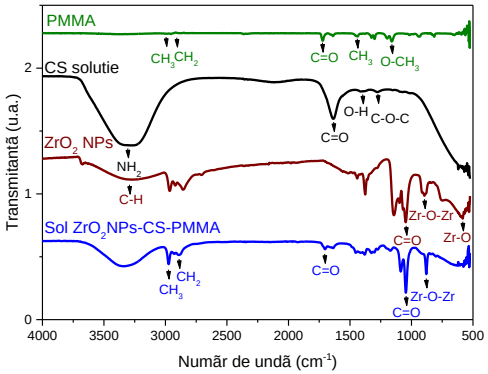

Fig. 3.1 FTIR spectrum of used precursors and ZrO_2 NPs-CS-PMMA hybrid sol

For the ZrO_2NPs-CS-PMMA sol, the peak corresponding to the absorption band from Zr-O-Zr is observed for the zirconium nanoparticles shifted from 895 to 878 cm-1, which highlights the presence of the zirconium ion interactions with the others. compounds. Also, the band corresponding to the amide I at the C = O bond of the chitosan shifted from 1634 to 1700 cm-1 is observed [115].

3.1.3 Morphology of hybrid films

The RMS roughness of the CS-PMMA film calculated on the surface of 2x2 μm using Gwyddion software has the value of 0.21 nm (Fig. 3.8).

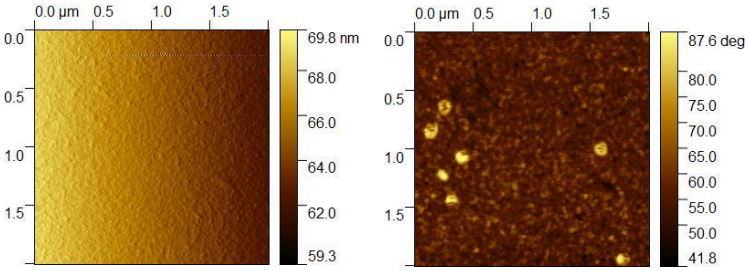

Fig. 3.8 AFM images for the two-layer CS-PMMA film. The 2D image (right) indicates the phase composition

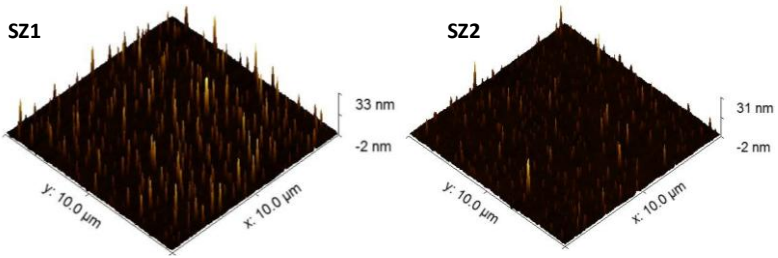

Fig. 3.9 AFM images for ZrO_2NPs-CS-PMMA films with one layer (SZ1) and two layers (SZ2). 2D images (middle) indicate the phase composition

The AFM images for both samples (Fig. 3.9), taken on a surface of 10 x 10 µm, show similar morphologies and indicate an RMS roughness of the hybrid films of 0.24 nm (SZ1) and 0.53 nm (SZ2).

3.1.4 Optical properties of hybrid films

From the optical spectrum of the films it is observed that in the case of the SZ1 sample, the transmittance value in the visible range is 91%, and for the SZ2 sample the value decreased to 88% (Fig. 3.12).

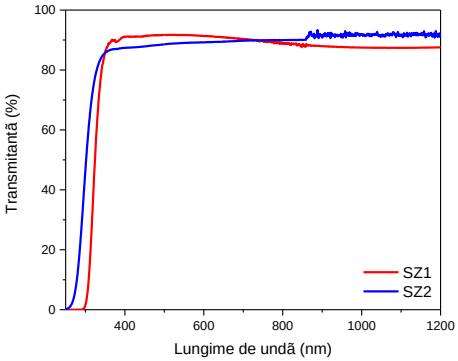

Fig. 3.12 Optical transmittance spectrum for ZrO_2NPs-CS-PMMA films with one layer (SZ1) and two layers (SZ2)

The yield values of band gap energy (Eg) and 3.645 eV to 3.551 eV sample SZ1 and SZ2 sample.

3.1.5 Electrical properties of hybrid films

The current density for hybrid films is constant at 1.3 A/cm^2 at the applied voltage between (-8V) - (- 4V) and decreases continuously with the decrease of voltage applied in the negative field, reaching and maintaining a zero value in the positive field of applied voltage (Fig. 3.18).

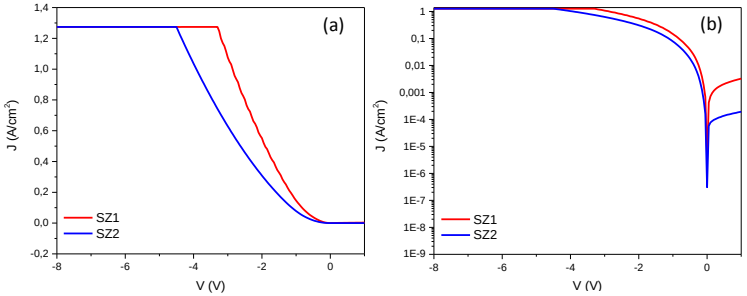

Fig. 3.18 The linear density characteristic (a) and logarithmic (b) voltage function for ZrO_2NPs-CS-PMMA films with one layer (SZ1) and two layers (SZ2)

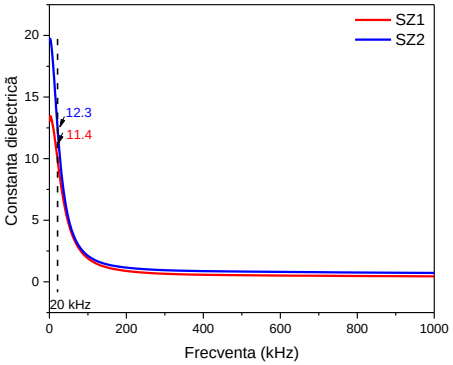

Fig. 3.21 The dielectric constant-frequency characteristic of ZrO_2NPs-CS-PMMA films with one layer (SZ1) and two layers (SZ2)

In the frequency dielectric constant curve for the ZrO_2NPs-CS-PMMA films, the dielectric constant values of 11.4 and 12.3 were obtained for the SZ1 and SZ2 samples, at the frequency of 20 kHz. These values are higher

compared to that obtained for the two-layer CS-PMMA film (8.8) and for the PMMA film (3.5) [119].

3.2 Thin films based on ZnONPs- CS-PMMA

3.2.3 Morphology of hybrid films

The SEM image of zinc oxide nanoparticles is shown in Fig. 3.26, noting that the nanoparticles are agglomerated.

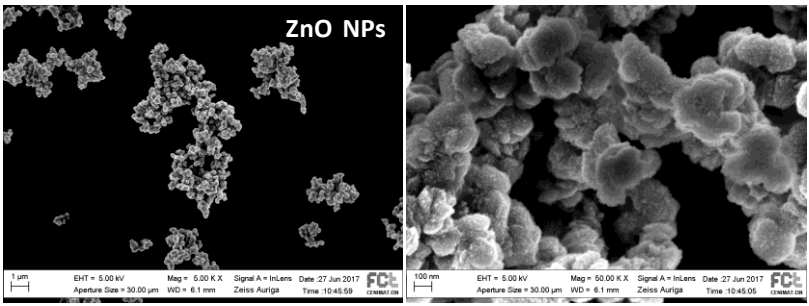

Fig. 3.26 SEM images of zinc oxide nanoparticles

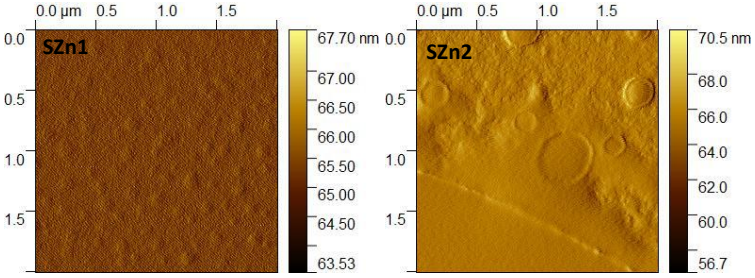

Fig. 3.28 AFM images for ZnONPs-CS-PMMA films with one layer (SZn1) and two layers (SZn2)

AFM images confirm the homogeneous distribution of nanoparticles in the polymer mass (Fig. 3.28). The RMS roughness value obtained for the SZn1 sample is 1.94 nm and increases to 2.79 nm for the SZn2 sample. A smoother and more uniform surface can be seen in SZn1 sample.

3.2.4 Optical properties of hybrid films

For both samples the transmittance value in the visible field is 90%. These high transmittance values indicate their use in transparent electronics (Fig. 3.29).

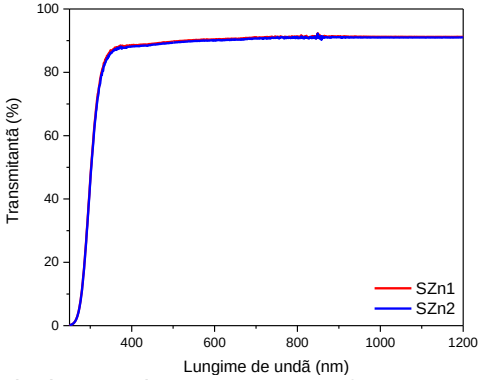

Fig. 3.29 Optical transmittance spectrum for ZnONPs-CS-PMMA films with one layer (SZn1) and two layers (SZn2)

Eg values of 3,543 eV were obtained for the SZn1 sample and 3,705 eV for the SZn2 sample. Eg value increases with increasing number of layers. These values of Eg indicate the applicability of the films obtained as a dielectric layer in the structure of a thin film transistor (TFT).

3.2.5 Electrical properties of hybrid films

The current density for ZnONPs-CS-PMMA hybrid films is constant with the value of 1.3 A / cm2 at an applied voltage between -8 and -6 V for the SZn2 sample and between -8 and -4 V for the SZn1 sample.

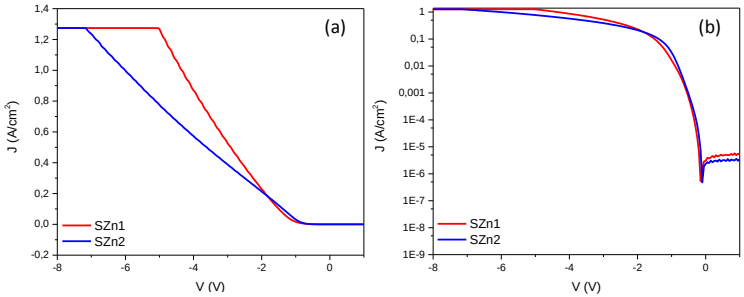

Fig. 3.31 The linear density characteristic (a) and logarithmic (b) voltage function for ZnONPs-CS-PMMA films with one layer (SZn1) and two layers (SZn2)

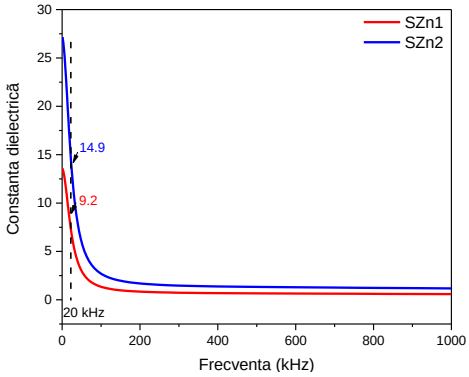

Fig. 3.34 The dielectric constant-frequency characteristic of ZnO NPs-CS-PMMA films with one layer (SZn1) and two layers (SZn2)

The value of the dielectric constant of the SZn1 sample is 9.2 and increases to 14.9 for the SZn2 sample, at the frequency of 20 kHz (Fig. 3.34). The higher value for the two-layer sample may be due to the increase in the number of hydroxyl groups as the film thickness increases.

3.3 Thin films based on Ag:ZnONPs-CS-PMMA

3.3.1 Chemical structure of precursors

In the PMMA spectrum the three characteristic peaks at 1158, 1442 and 1723 cm-1 attributed to the O-CH3, CH3 and C = O connections are observed [113]. The peaks from 1634 and 1390 cm-1, attributed to the amide I and amide II bands of chitosan, confirms deacetylation of the polymer (75-85%) [115].

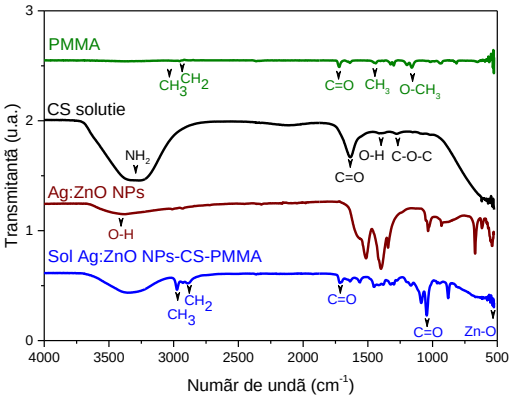

Fig. 3.35 FTIR spectrum of the precursors used and the sol obtained by Ag: ZnO NPs-CS-PMMA

In the case of the sol Ag:ZnO NPs-CS-PMMA spectrum an increase in peak intensity can be seen. The shift of the peak attributed to the amide I band of the chitosan to higher energy values from 1634 cm-1 to 1652 cm-1 may be due to the chemical interactions that take place between chitosan and the other compounds [122].

3.3.3 Morphology of hybrid films

In SEM images of silver doped zinc oxide nanoparticles shown in Fig. 3.39 agglomerates of nanoparticles can be observed.

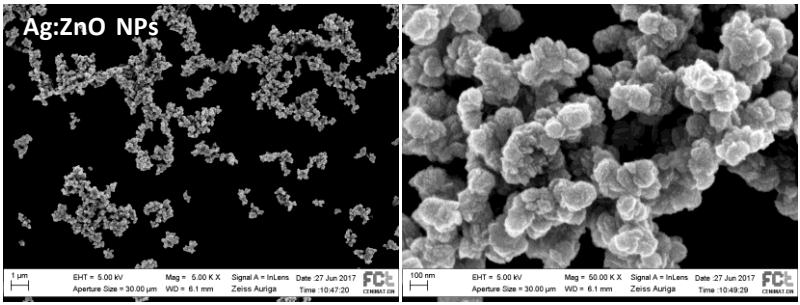

Fig. 3.39 SEM images of silver doped zinc oxide nanoparticles

The SEM images of the hybrid films show the distribution of Ag:ZnO nanoparticles in the chitosan matrix and PMMA throughout the examined surface and agglomerations of Ag:ZnO nanoparticles in the two-layer sample (SAZn2) (Fig. 3.40).

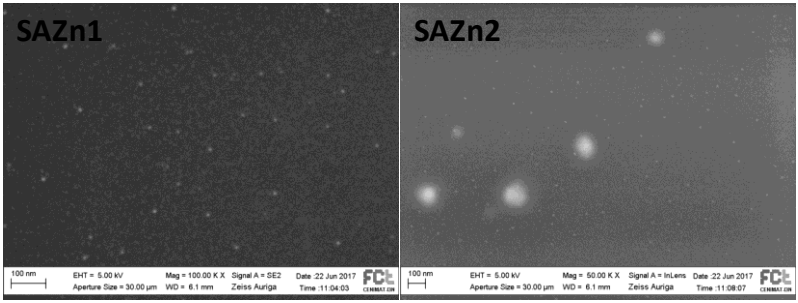

Fig. 3.40 SEM images for Ag films: ZnO-CS-PMMA with one layer (SAZn1) and two layers (SAZn2)

From the AFM images (Fig. 3.41) indicating the phase composition, a uniform distribution of Ag: ZnO nanoparticles is observed in the chitosan and PMMA matrix, in agreement with the SEM images. The RMS roughness value decreased from 1.58 nm for the one-layer sample (SAZn1) to 0.442 nm for the two-layer sample (SAZn2).

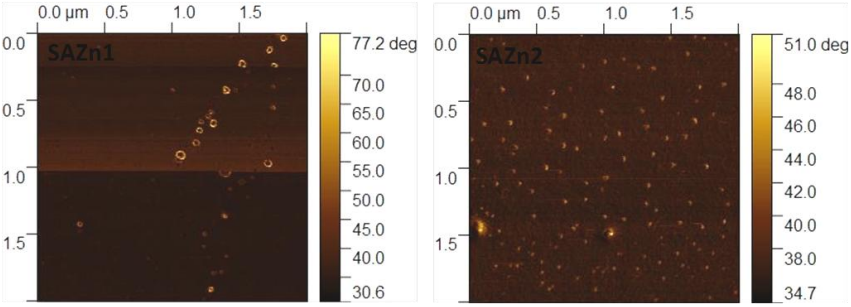

Fig. 3.41 AFM images for Ag films: ZnO NPs-CS-PMMA with one layer (SAZn1) and two layers (SAZn2)

3.3.4 Optical properties of hybrid films

For both samples the transmittance value in the visible range is 90% (Fig. 3.42). These high transmittance values allow their use in transparent electronics.

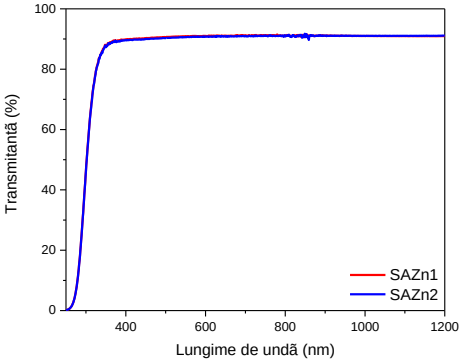

Fig. 3.42 Optical transmittance spectrum for Ag films: ZnO NPs-CS-PMMA with one layer (SAZn1) and two layers (SAZn2)

From the obtained values of the optical transmittance, the energy values of the forbidden band (Eg) were calculated and the value of 3.737 eV and 3.638 eV for the SAZn2 sample were obtained for the SAZn1 sample.

3.3.5 Electrical properties of hybrid films

The current density has a constant value of 1.3 A/cm^2 at the applied voltage between (-8V) - (- 4V) for the SAZn2 sample and between (-8V) - (- 1V) for the SAZn1 sample, becoming null at positive values of the voltage applied for both samples (Fig. 3.44).

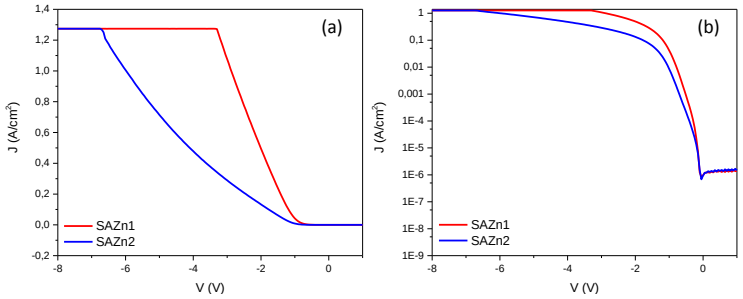

Fig. 3.44 The linear density characteristic (a) and logarithmic (b) voltage function for the Ag films: ZnONPs-CS-PMMA with one layer (SAZn1) and two layers (SAZn2)

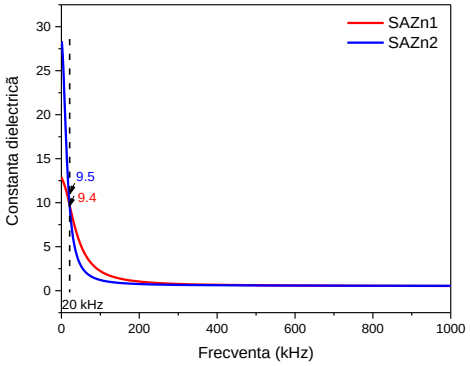

Fig. 3.47 The dielectric constant-frequency characteristic of Ag films: ZnO NPs-CS-PMMA with one layer (SAZn1) and two layers (SAZn2)

The value of the dielectric constant at the frequency of 20 kHz is 9.4 for the SAZn1 sample and 9.5 for the SAZn2 sample (Fig. 3.47).

CHAPTER 4

CONTRIBUTIONS TO THE OBTAINING OF THE HYBRID MATERIALS BASED ON CHITOSAN IN ACRYLIC MATRIX

In this chapter, the experimental results regarding the morphological, structural and thermal characterization of hybrid materials with chitosan in acrylic matrix are presented for applications in prosthetics.

Two series of hybrid materials were obtained by mixing the commercial acrylic matrix Duracryl Plus with chitosan solution. The effect of concentration and the order of addition of chitosan solution in the acrylic matrix on the morphology, structure and thermal properties of the obtained hybrid materials was analyzed.

4.1 Structure and morphology

4.1.1 Structure of the precursors and obtained hybrid materials

Duracryl® Plus powder (P) consists of methylmethacrylate-methacrylate copolymer (MMA-co-MA), in the form of microspheres, in greater than 95% and 1-5% dibenzoyl peroxide (DBP), and the liquid component (L) contains methylmethacrylate (MMA) 85-90% and dimethyl-

paratoluidine (DMPT) <5% [123]. When the microspheres are introduced into the liquid, upon contact with the DBP polymerization initiating agent, the MMA monomer polymerizes and forms a transparent solid film of polymethylmethacrylate (PMMA), according to the chemical reaction (1), which includes the MMA-co-MA microspheres and forms a cross-linked hybrid composite material.

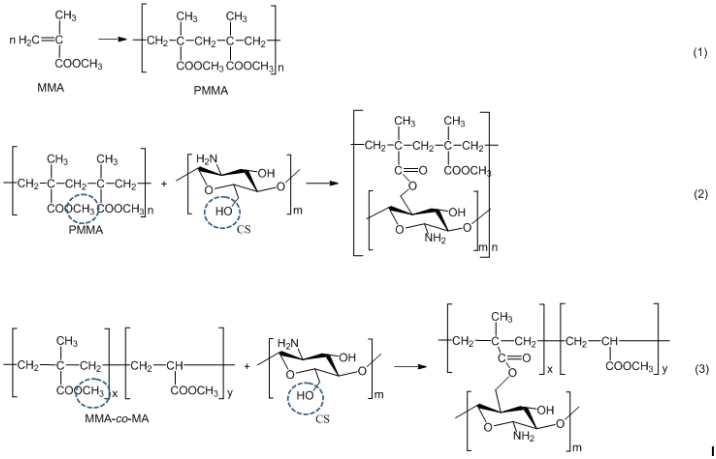

Equations of the proposed chemical reactions for the processes of obtaining the hybrid material

While acrylic monomers have carbon double bonds (C = C) and methoxy groups (-OCH3), which can interact with each other or with other reactants by polymerization (chemical reaction 1) and / or condensation, PMMA and MMA-co polymers. -MA have only methoxy reactive groups (encircled in chemical reactions 2 and 3) which lead to condensation reactions.

4.1.2 Morphology of the obtained hybrid materials

In the SEM images of the hybrid materials (Fig. 4.7) it is observed that grafting of chitosan on acrylic resin takes place on the surface of the MMA-co-MA spheres when the chitosan solution was added before mixing the acrylic components (sample Ac 2-2) or on the film PMMA polymer exterior when the chitosan solution was added after mixing the acrylic components (sample Ac 1-2), being in correlation with the FTIR spectra.

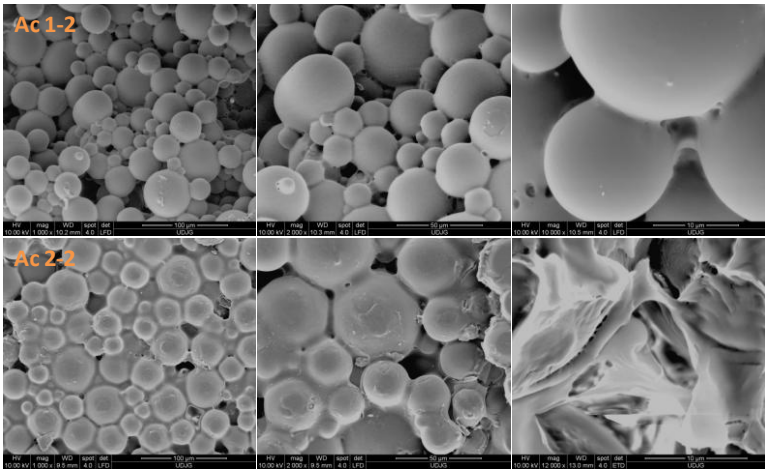

Fig. 4.7 SEM images of hybrid materials with chitosan added after (Ac 1-2) and before (Ac 2-2) by mixing the acrylic components

4.2 Thermal behavior of the obtained hybrid materials

The character of the DSC curves for the hybrid samples is different compared to the reference acrylic matrix (Fig. 4.17). In the case of Ac 1-1 sample, two endothermic processes and two exothermic processes are observed.

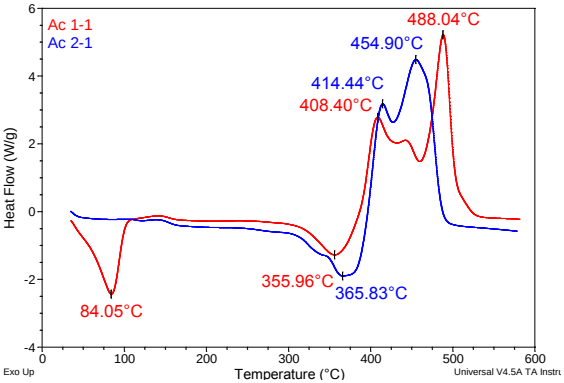

Fig. 4.17 DSC curve of hybrid materials with chitosan added after (Ac 1-1) and before (Ac 2-1) by mixing the acrylic components

In the case of Ac 2-1, the first endothermic process disappears, and the peaks are shifted to higher values compared to the Ac 1-1 sample, with the exception of the last exothermic process corresponding to the thermal decomposition of chitosan.

The DSC (Rev HF) curve associated with the physical transformations of the acrylic chitosan-matrix hybrid materials is shown in Fig. 4.20. In case of Ac 1-1 sample, the peak corresponding to the endothermic

process of water evaporation with the chemical breakdown of the hydroxyl groups from the C3 and C6 carbons or the NH2 group of the chitosan is observed, being shifted to lower values compared to the film. of chitosan.

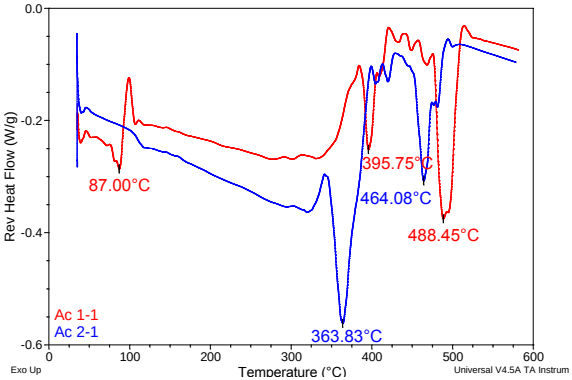

Fig. 4.20 DSC curve in reversible heat flux (Rev HF) of hybrid materials with chitosan added after (Ac 1-1) and before (Ac 2-1) by mixing the acrylic components

The DSC curve (Nonrev HF) associated with the chemical transformations that occur in the obtained hybrid materials is shown in Fig. 4.23.

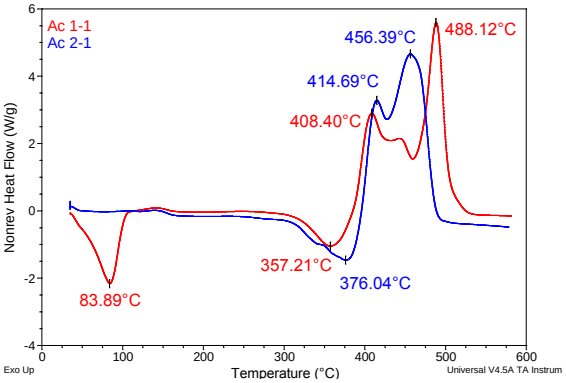

Fig. 4.23 DSC curve in irreversible heat flux (Nonrev HF) of hybrid materials with chitosan added after (Ac 1-1) and before (Ac 2-1) by mixing the acrylic components

For all hybrid samples, endothermic chemical processes (200-370 °C) are shifted to higher values and exothermic processes (400-480 ° C) are shifted to lower values, compared to that of chitosan film, which can be explained. by eliminating the acetyl group and / or depolymerizing the chitosan associated with the oxidation process in air. At the same time, it can be observed that the chitosan increases the thermal stability of the acrylic matrix, highlighting the chemical interaction that takes place between the chitosan and the acrylic matrix.

CHAPTER 5
CONTRIBUTIONS TO OBTAINING HYBRID MATERIALS BASED ON OXIDE NANOPARTICLES EMBEDDED IN CHITOSAN AND ACRYLIC MATRIX

In this chapter, the experimental results regarding the morphological, structural, thermal and antimicrobial characterization of hybrid materials based on chitosan oxide nanoparticles and acrylic matrix for prosthetics are presented.

Four series of hybrid materials were obtained by mixing the Duracryl Plus commercial acrylic matrix with ZnO and Ag: ZnO nanoparticles and ZnO/CS and Ag:ZnO/CS composite nanoparticles. The effect of the concentration and of the different types of oxide and composite nanoparticles in acrylic matrix on the morphology and structure and the thermal and antimicrobial properties of the obtained hybrid materials is analyzed.

5.2 Mechanisms of formation of hybrid materials

In the chemical reaction below, a proposed scheme for the chemical interactions between the composite nanoparticles (ZnO/CS and Ag:ZnO/CS) and the cross-linked acrylic matrix in the formation of the hybrid material is presented.

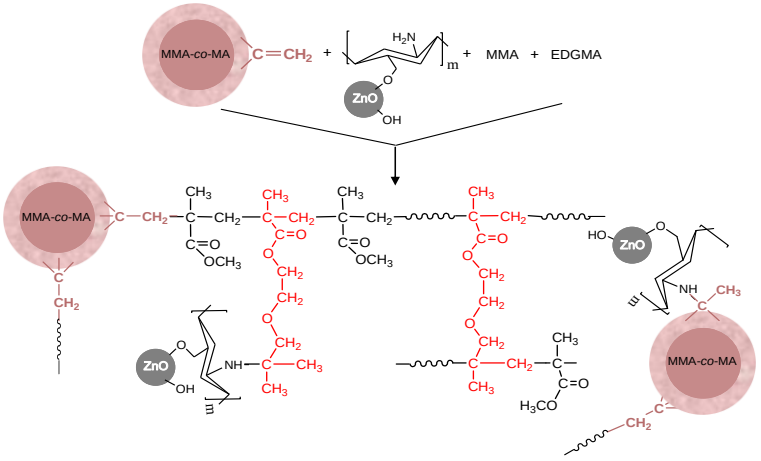

This reaction involves amine grouping of chitosan and vinyl grouping of the acrylic matrix or that of the EGDMA crosslinking agent molecule present in the Duracryl Plus commercial resin.

5.3 Morphology of the obtained hybrid materials

In the SEM images of the hybrid materials shown in Fig. 5.3 a compact arrangement of the microspheres of the acrylic matrix copolymer is observed and a relatively good dispersion of the nanoparticles in the acrylic matrix with dimensions between 100-300 nm (NPs without chitosan) and 60-200 nm (NPs with chitosan). Agglomerations of nanoparticles are also observed for AcZ1 and AcAZ1 hybrid materials.

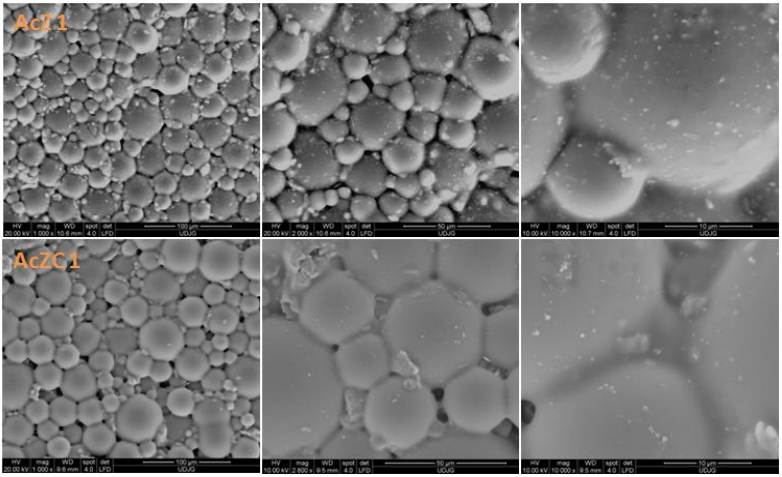

Fig. 5.3 SEM images of hybrid materials based on ZnO (AcZ1) nanoparticles and ZnO/CS composite nanoparticles (AcZC1) in acrylic matrix

5.4 Thermal behavior of the precursors and obtained hybrid materials

The variation of activation energy during the two main decomposition stages of the investigated samples AcZC1 and AcAZC1 is indicated by circle and arrow (Fig. 5.11). It can be observed that in the case of hybrid materials, the activation energy has lower values for the first decomposition stage and for the second decomposition stage it registers higher values, compared to those of the reference acrylic material (Ac0).

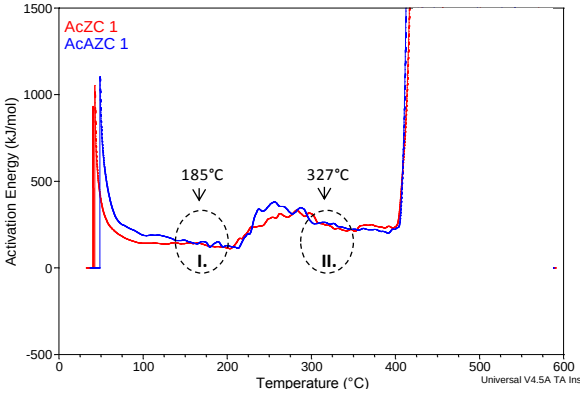

Fig. 5.11 Activation energy of hybrid materials with ZnO/CS composite nanoparticles (AcZC1) and Ag:ZnO/CS (AcAZC1)

The software associated with the differential scanning calorimetry technique, which can separate the reversible and irreversible kinetic events, allowed the total heat flux (HF, Fig. 5.13) to be decomposed into the irreversible heat flux (nonrev HF, Fig. 5.15) associated with the reactions. kinetically controlled irreversible chemicals and reversible heat flux (rev HF, Fig. 5.17) associated with reversible physical transformations. Thus, we can assume that between temperatures 30 and 120 ° C, the endothermic process of chemical breakdown of hydroxyl groups from groups C3 and C6 overlaps with the endothermic process of evaporation of the resulting water [138-140]. In the second step of decomposition (200-350 ° C) the physical endothermic process (peak HF rev) and the

exothermic kinetic process (peak non-HF) can be explained by elimination of acetyl groups and/or depolymerization of the associated chitosan [122,131]. with oxidative degradation.

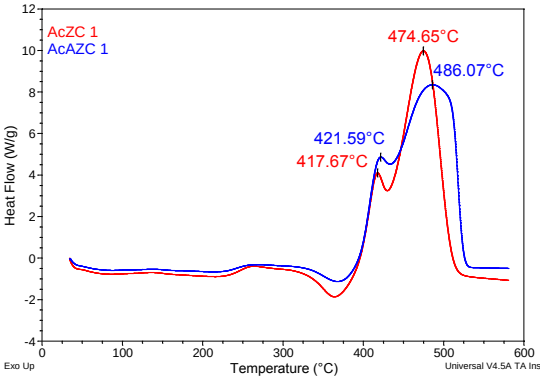

Fig. 5.13 DSC curve of hybrid materials with ZnO/CS composite nanoparticles (AcZC1) and Ag:ZnO/CS (AcAZC1)

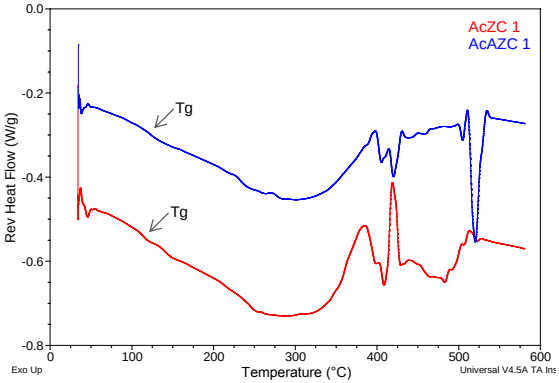

Fig. 5.17 Reversible heat flux of hybrid materials with ZnO/CS composite nanoparticles (AcZC1) and Ag:ZnO/CS (AcAZC1)

5.5 Antimicrobial activity of the obtained hybrid materials

Figure 5.19 shows the results of the dark zone inhibition test for evaluating the antibacterial activity of the modified hybrid materials with different concentrations of Ag:ZnO and Ag:ZnO/CS nanoparticles compared to the activity of the unmodified acrylic material, against two types of bacteria, *S aureus* gram-positive and gram-negative more resistant *E. coli.*

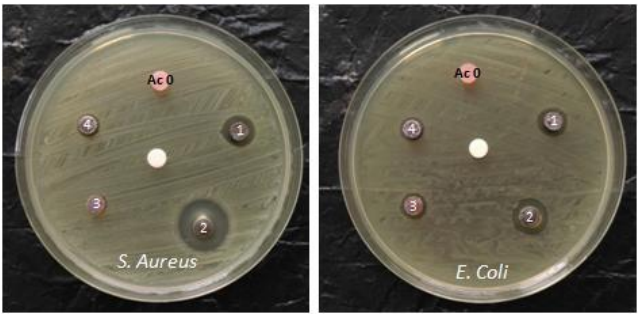

Fig. 5.19 Antimicrobial activity on S.Aureus and E.Coli bacteria of the reference acrylic matrix (Ac 0) and hybrid materials with Ag: ZnONPs: AcAZ1 (1) and AcAZ2 (2) and with Ag:ZnO/CS NPs: AcAZC1 (3) and AcAZC2 (4)

In Figure 5.19, it can also be observed that the value of nanoparticle concentration has a more pronounced effect on the antimicrobial activity of chitosan-free materials (AcAZ1 and AcAZ2) than in the case of chitosan grafted Ag: ZnO / CS NPs (AcAZC1 and AcAZC2).

CHAPTER 6

CONTRIBUTIONS TO OBTAINING CHITOSAN-HAP BIOMIMETIC HYBRID COATINGS

In this chapter, the experimental results regarding the morphological, structural and mechanical characterization of the biomimetic hybrid coatings based on chitosan and hydroxyapatite are presented.
Two series of hybrid biomimetic coatings were obtained in the presence of commercial hydrogel Emdogain (first series) and mixed hydrogel Emdogain-chitosan (second series). The effect of the used hydrogel and the influence of the growth time in artificial saliva on the morphology, structure and mechanical properties were investigated.

6.1 Structure of biomimetic coatings

6.1.1 Crystalline structure

From the XRD diffractograms, it can be observed that the remineralized samples without CS (Fig. 6.2) show peaks characteristic of the HAP hexagonal phase. However, some of the major HAP diffraction peaks are obscure, which also indicates the presence of the amorphous phase. The presence of hydroxyapatite crystals with hexagonal structure is also confirmed in the case of samples obtained in the presence of the hydrogel with CS (Fig. 6.3).

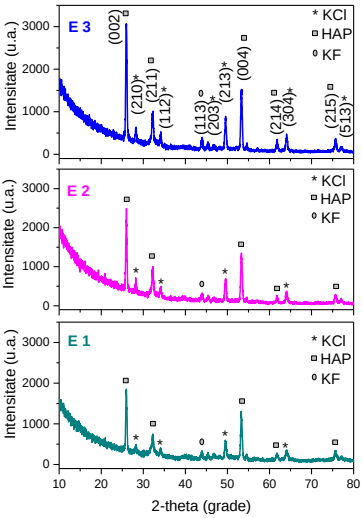

Fig. 6.2 X-ray diffractogram of biomimetic layers increased in the presence of EMD hydrogel for 4 (E1), 7 (E2) and 10 days (E3)

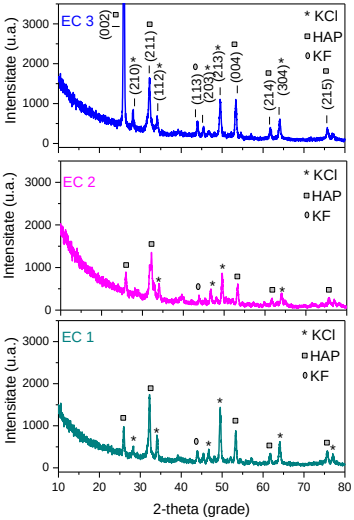

Fig. 6.3 X-ray diffractogram of biomimetic layers increased in the presence of the EMD-CS hydrogel for 4 (EC1), 7 (EC2) and 10 days (EC3)

6.1.2 Chemical structure

In the case of the remineralized samples in the presence of the EMD hydrogel (Fig. 6.5), the intensity of the hydroxyapatite bands (HAP) is observed. The positions of the bands for the PO43- link are shifted to higher values in the case of the second series of remineralized samples in the presence of the CS-EMD hydrogel (Fig. 6.6), indicating that the interactions between the CS and PAH are present.

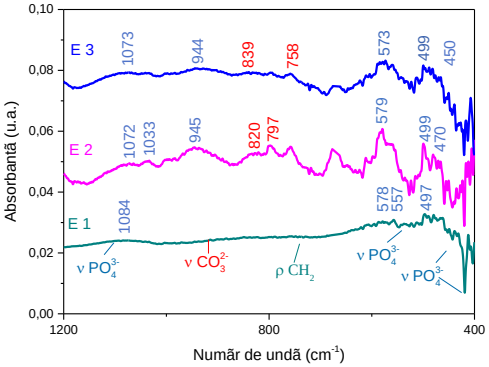

Fig. 6.5 FTIR spectrum of biomimetic layers increased by maintaining in artificial saliva for 4 (E1), 7 (E2) and 10 days (E3), in the presence of the hydrogel with EMD

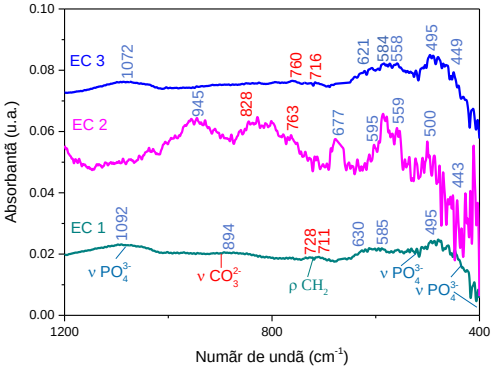

Fig. 6.6 FTIR spectrum of biomimetic layers increased by maintenance in artificial saliva for 4 (EC1), 7 (EC2) and 10 days (EC3), in the presence of the EMD-CS mixed hydrogel

In the RAMAN spectra (Figures 6.8-6.9) we observe the types of connections of the PO43- group at 960 cm-1 (v1), 420-450 cm-1 (v2), 1000-1100 cm-1 (v3), 580-610 cm-1 (v4), of the CO32- group at 1070 cm-1 (v1) and of the stretching linkage v (OH) at about 3570 cm-1 specific for carbonated hydroxyapatite [158].

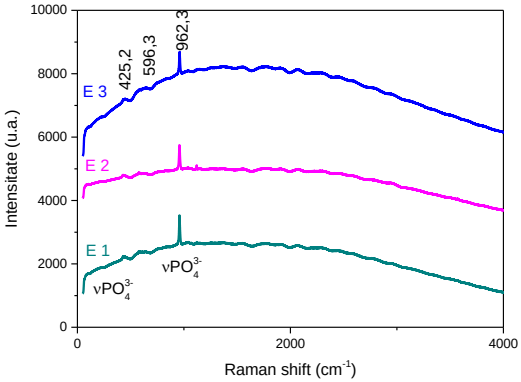

Fig. 6.8 RAMAN spectrum of biomimetic layers increased in the presence of EMD hydrogel maintained in artificial saliva for 4 (E1), 7 (E2) and 10 days (E3)

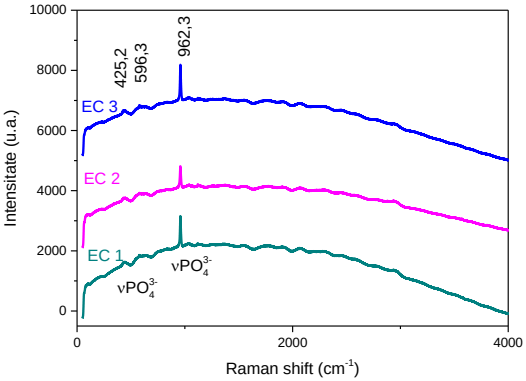

Fig. 6.9 RAMAN spectrum of biomimetic layers increased in the presence of EMD-CS mixed hydrogel maintained in artificial saliva for 4 (EC1), 7 (EC2) and 10 days (EC3)

6.2 Morfology of biomimetic layers

The morphology of the biomimetic layers shows an increase in the length of the newly developed nanocrystals in the case of E1-E2 samples. When the retention time increases from 7 to 10 days the morphological change of the crystals and the formation of outer spherical particles takes place (Fig. 6.12) [163-165].

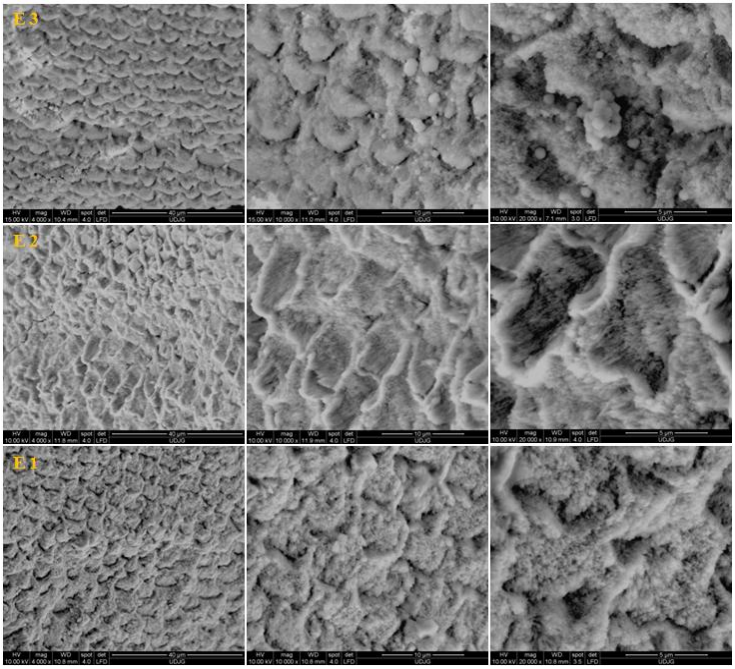

Fig. 6.12 SEM images of biomimetic layers grown in the presence of EMD hydrogel maintained in artificial saliva for 4 (E1), 7 (E2) and 10 days (E3)

Figure 6.13 shows significant morphological changes for the remineralized samples in the presence of the EMD-CS hydrogel, compared to the remineralized samples without chitosan.

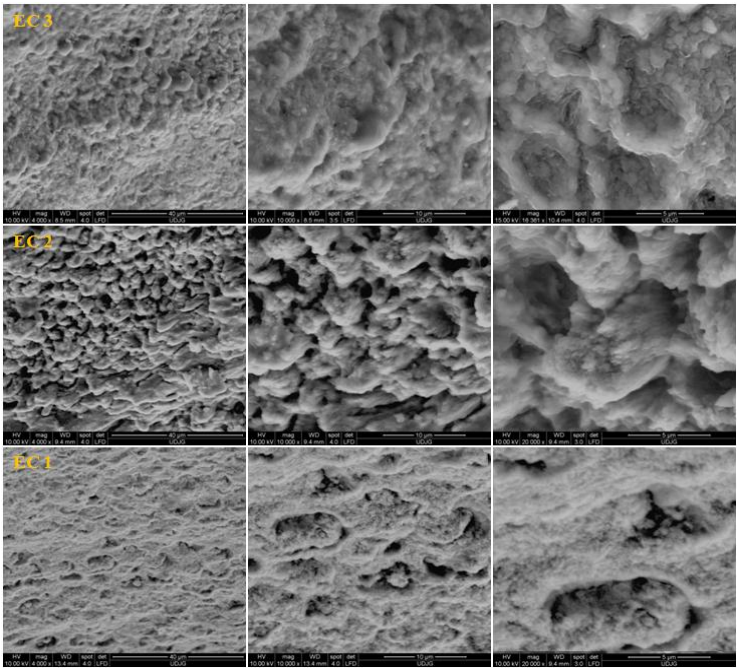

Fig. 6.13 SEM images of the biomimetic layers grown in the presence of the EMD-CS hydrogel maintained in artificial saliva for 4 (EC1), 7 (EC2) and 10 days (EC3)

6.3 Mechanical properties of coatings

The hardness behavior shown in Fig. 6.15 is different for remineralized samples with or without CS. Thus, compared with the hardness of the demineralized sample (R0), the hardness of the remineralized samples in the presence of the EMD hydrogel for 4-10 days (samples

E1-E3) increased from 41-58% for samples E1-E2 and up to 81-92% for sample E3, while for samples remineralized in the presence of the EMD-CS hydrogel it increased by 29.6 and 32.5% for samples EC1 and EC2 and decreased by 13.3% for sample EC3. A significant decrease in hardness value was observed for the remineralized sample for 10 days using the EMD-CS hydrogel (EC3).

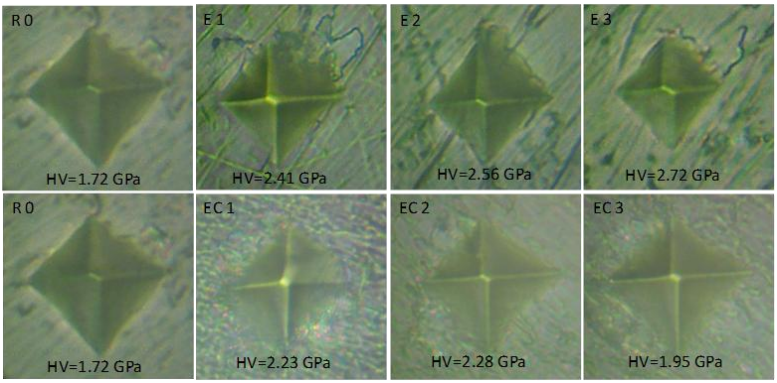

Fig. 6.15 Optical microscopy images of the measurements of the micro-hardness of the demineralized substrate (R0) and of the increased biomimetic layers in the presence of the EMD hydrogel (E1-E3) and the EMD-CS hydrogel (EC1-EC3) for 4, 7 and 10 days

CHAPTER 7

GENERAL CONCLUSIONS, PERSONAL CONTRIBUTIONS AND FUTURE RESEARCH DIRECTIONS

The main objective of the study presented in this paper was to obtain and characterize complex multifunctional hybrid systems, in the form of solid thin films, biomimetic coatings and profiled materials based on natural biopolymers (CS) and synthetic biocompatible polymers (PMMA) with or without oxide nanoparticles. , for applications in the field of transparent and / or flexible electronics and in biomedical fields.

Following the studies and research carried out, the conclusions presented below were highlighted.

On obtaining thin films based on oxide nanoparticles embedded in chitosan and PMMA

- Three thin hybrid film systems based on oxide nanoparticles (ZrO2, ZnO and Ag: ZnO) were obtained from the modified sol-gel method and were characterized morphologically, structurally, thermally, optically and electrically by chitosan and PMMA, with one layer and two layers.
- The precursor soils used to obtain the hybrid films were characterized by FTIR spectroscopy, highlighting the presence of the components

mentioned above and the strong chemical interaction between them.

- The capacity value decreases with increasing thickness for ZrO2NPs-CS-PMMA hybrid film systems (from 1300 nF / cm2 to 300 nF / cm2) and Ag: ZnONPs-CS-PMMA (from 1150 nF / cm2 to 300 nF / cm2) and increases slightly for ZnONPs-Cs-PMMA films (from 700 nF / cm2 for 1 layer to 750 nF / cm2 for 2 layers) at the applied voltage of -3V.
- All thin films have high values of dielectric constant, at the frequency of 20 kHz; the highest and the lowest values were obtained for the Ag: ZnONPs-CS-PMMA film with one layer (14.9), and for the ZnONPs-Cs-PMMA film with one layer (9.2) respectively.

On obtaining chitosan-based hybrid materials in acrylic matrix

- Two series of hybrid materials based on self-curing dental acrylic resins (Duracryl® Plus) grafted with chitosan were prepared. The effect of chitosan concentration and how it was added to the acrylic resin components on the thermal behavior, morphology and structure of the resulting hybrid materials was studied.
- Hybrid materials were characterized by FTIR spectroscopy, highlighting the chitosan grafting on the surface of the MMA-co-MA (acrylic powder) copolymer spheres when chitosan was added before mixing the acrylic components (powder and

liquid) and on the outer polymer film. PMMA when chitosan was added after mixing the acrylic components.

- The hybrid materials obtained have a compact morphology (SEM) consisting of MMA-MA microspheres aggregated through a CS-PMMA hybrid film. As the chitosan concentration increases and it is added after mixing the solid and liquid acrylic components, the porosity of the resulting hybrid material increases.
- Thermal analysis of all samples highlights the increased thermal stability of the acrylic matrix following the addition of chitosan.
- The thermal stability of the hybrid materials varies depending on the mass ratio between chitosan and the liquid component of Duracryl and the order of mixing of the components.
- TG-DTG-DSC curves indicate the presence of three stages of thermal decomposition of CS-PMMA hybrid materials in air, between 25-600 ° C.
- All samples show a partial overlap of the physical and chemical processes in the range 300-400 ° C, corresponding to the elimination of the acetyl group. In the 500-600 ° C range, a perfect overlap of an exothermic chemical process with an endothermic physical one was observed corresponding to the oxidative decomposition of chitosan in air and the elimination of the resulting components.

On obtaining hybrid materials based on chitosan oxide nanoparticles and acrylic matrices

- Four series of hybrid materials based on self-curing dental acrylic resins (Duracryl® Plus) containing ZnO and Ag:ZnO and ZnO/CS and Ag:ZnO/CS composite nanoparticles were prepared and characterized morphologically, structurally, thermally and antimicrobially..
- Hybrid materials modified with nanoparticles have a compact arrangement of acrylic copolymer microspheres with good contact between them, good dispersion of nanoparticles with dimensions between 100-300 nm (oxide nanoparticles, without chitosan) and 60-200 nm (composite nanoparticles oxide-chitosan) and good adhesion of the nanoparticles to the copolymer microspheres.
- Incorporation of composite nanoparticles into hybrid materials increased the temperature T50% (temperature to 50% mass loss) by about 50 ° C in air, indicating strong chemical interactions between components.
- The resulting hybrid materials show higher values of the activation energy of the thermal decomposition processes, compared to the reference acrylic material, explaining the increase of the thermal stability of the first ones by the presence of strong chemical interactions between the components.
- Hybrid materials modified with Ag:ZnO and Ag: ZnO/CS nanoparticles exhibit good antibacterial

activity against S. aureus and E. coli bacteria, the strongest activity being observed for the material wit Ag: ZnO nanoparticles against E. coli.

On obtaining hybrid coatings biomimetic chitosan-HAP

- Two series of hybrid coatings were obtained on demineralized natural enamel substrates by the biomimetic growth of hydroxyapatite layers in the presence of commercial Emdogain based hydrogels (first series) and commercial Emdogain and chitosan based (second series). The effect of the hydrogel used and the influence of the growth time of the biomimetic layers by immersion in artificial saliva, on the morphology, structure and mechanical properties of the obtained hybrid coatings were studied.
- The coatings obtained are mainly composed of acicular crystals of hydroxyapatite, the main inorganic component of the natural enamel.
- The average size of PAH crystallites from the biomimetic coatings obtained in the presence of EMD hydrogel and in the presence of EMD-CS is larger than those of the crystallites in the demineralized enamel used as substrate.
- In the case of the remineralized layers in the presence of the EMD hydrogel, the length of the newly formed PAH nanocrystals increases with the increase of the immersion period in saliva from 4 to 7 days. The morphological and structural changes

produced by increasing the remineralization duration from 7 to 10 days indicate a change in the appearance of crystals and the appearance of specific fluoroapatite formations.

- The samples remineralized in the presence of the EMD hydrogel (series I) show a monotonous increase of the micro-hardness with the increase of the retention time in saliva, between 4-10 days, whereas for the samples remineralized in the presence of the EMD-CS hydrogel, the micro-hardness increases from 4 and 7 days and decreases more sharply for the 10-day growth period, mainly due to the increase of the chitosan content and the decrease of the carbonate ion content in the surface layer.

Personal contributions

The personal contributions in the realization of this thesis consisted of:

- Obtaining new hybrid nanostructured dielectric materials based on oxides (ZrO2, ZnO and Ag: ZnO) and polymers (chitosan and PMMA), in the form of thin films.
- Obtaining dielectric hybrid thin films with high capacitance values (1200 nF) at temperatures below 200 ° C.
- Obtaining new hybrid materials based on chitosan and oxide nanoparticles (ZnO and Ag:ZnO) and

composite nanoparticles (ZnO / CS and Ag: ZnO / CS) in acrylic matrix.

- ❖ Highlighting the use of oxide nanoparticles to improve antimicrobial properties.
- ❖ Obtaining biomimically enhanced layers on chitosan-PAH enamel substrate.

Future research directions

- Optimization of the post-deposition treatment and the number of layers of hybrid films based on oxide nanoparticles in chitosan and PMMA in order to improve the dielectric properties;
- Incorporating dielectric hybrid films into thin film based transistors;
- Toxicity analysis of the obtained hybrid dental materials;
- Study of the influence on the morphology and mechanical properties of dental hybrid materials immersed in artificial saliva;
- Growth of hybrid layers based on oxide nanoparticles on demineralized tooth enamel substrate.

List of works published and presented at scientific events

Published works

1. Ghisman Pleșcan Viorica, Viorica Mușat, Ana Pimentel, Tomas R.Calmeiro, Emanuel Carlos, Liliana Baroiu, Rodrigo Martins, Elvira Fortunato, Hybrid (Ag)ZnO/Cs/PMMA nanocomposite thin films, Journal of Alloys and Compounds, 803 (2019) 922-933, **ISI, IF (2018)- 4.175**

2. Agripina Zaharia, Viorica Muşat, Elena Maria Anghel, Irina Atkinson, Oana-Cătălina Mocioiu, Mariana Buşilă, **Viorica Ghisman Pleşcan**, Biomimetic chitosan-hydroxyapatite hybrid biocoatings for enamel remineralization, Ceramics International, 43 (2017) 11390–11402, **ISI, IF (2016)-2.986**

3. Agripina Zaharia, **Viorica Ghisman Pleșcan**, Elena Maria Anghel, Viorica Musat, Human Dentine Remineralization Under Non-colagen Materials Action, Revista de Chimie, 68, no. 5 (2017) 928-932, **ISI**, **IF (2016)-1.232**

4. Agripina Zaharia, **Viorica Ghisman Pleșcan**, Irina Atkinson, Oana Catalina Mocioiu, Alina Cantaragiu, Viorica Musat, Remineralization of Natural Tooth Enamel in Artificial Saliva Environment, Revista de Chimie, 68, no. 3 (2017) 510-514, **ISI**, **IF (2016)-1.232**

5. Agripina Zaharia, Viorica Mușat, **Viorica Pleșcan Ghisman**, Nicușor Baroiu, Antimicrobial hybrid biocompatible materials based on acrylic copolymers modified with (Ag)ZnO/chitosan composite nanoparticles, European Polymer Journal 84 (2016) 550–564, **ISI**, **IF (2016)-3.485**

6. Agripina Zaharia, **Viorica Pleșcan Ghisman**, Corina Laura Ștefănescu, Viorica Mușat, Thermal, morphological and structural characterization of chitosan-modified hybrid materials for prosthodontics, Rev. Chim., 67/10 (2016), **ISI, IF (2015)-0.956**

Works presented at scientific events

1. Viorica Ghisman Pleșcan, Agripina Zaharia, Elena Maria Anghel, Irina Atkinson, Oana Catalina Mocioiu, Mariana Bușilă, Viorica Mușat, Chitosan-hydroxyapatite nanocomposite layers for enamel remineralization, 14th International Conference on Nanosciences & Nanotechnologies, 4-7 iulie 2017, Thessaloniki, Greece, poster P3-21, la Workshop 3 –Nanomedicine

2. Elena Emanuela Herbei, **Viorica Pleșcan (Ghisman)**, Susane Oertel, Daniel Timpu, Michael P.M. Jank, Viorica Musat, Thermal behaviour and dielectric properties of ZrO_2-PMMA hybrid systems and spin-coated thin films, 14th International Conference on Nanosciences & Nanotechnologies, 4-7 iulie 2017, Thessaloniki, Greece, poster P1-3, la Workshop 1 –Plasmonics-Nanoelectronics & Clean Energy

3. Viorica Pleșcan (Ghisman), Petrică Alexandru, Andreea Dediu, Mariana Bușilă, Viorica Mușat, Thermal and Mechanical Properties of Hybrid Materials Based on Acrylic Resins Modified with Chitosan and ZnO/Chitosan Nanoparticles, Conferința Școlilor Doctorale CSSD-UDJG, 8-9 iunie 2017, Galați, ediția a V-a, poster P.P.3.6

4. Agripina Zaharia, Mariana Buşilă, Irina Atkinson, Elena Maria Anghel, Oana Cătălina Mocioiu, **Viorica Ghisman Pleşcan** and Viorica Muşat, Effect of chitosan on the regeneration of tooth enamel using emdogain gel bioactive template, Conferință Internationala de Chimie fizica ROMPHYSCHEM 16, 21-23 septembrie 2016, Galati, Romania : poster la sectiunea 8

5. Viorica Pleşcan (Ghisman), Mariana Buşilă, Petrică Alexandru, Andreea Dediu, Rodica Dinică, Viorica Muşat, Effect of chitosan properties of the thermal and mechanical properties of some composite materials with acrylic matrix, Conferința Școlilor

Doctorale CSSD-UDJG, 2-3 iunie 2016, Galați, ediția a IV-a, prezentare orală -**premiul III**

6. Agripina N. Zaharia, Corina Laura Ştefănescu, **Viorica Ghisman**, Mariana Ibănescu, Viorica Muşat, Thermal stability and mechanical behavior of some hybrid biocompatible materials for prosthodonties (poster), Scientific Conference of Doctoral Schools from UDJ Galati, România, Third Edition, 4-5 iunie 2015

7. Viorica Pleșcan (Ghisman), Elena Emanuela Herbei, Silviu Epure, Laurențiu Frangu, Alexandru Petrică, Țimpu Daniel, Viorica Musat, Hybrid nanomaterials as dielectric gate for thin films transistors (prezentare orală), Scientific Conference of Doctoral Schools from UDJ Galati, România, Third Edition, 4-5 iunie 2015- **premiul III**

Selective bibliography

[1] W.H. Binder, *The past 40 years of macromolecular sciences: reflections on challenges in synthetic polymer and material science*, Macromolecular Rapid Communications 40(1) (2019) 1800610.

[79] P. Gómez-Romero, C. Sanchez (Eds.) *Functional Hybrid Materials*, Wiley-VCH, 2004, Weinheim, ISBN 3-527-30484-3.

[80] E. Ruiz-Hitzky, P. Aranda, M. Darder, in CRC Concise Encyclopedia of Nanotechnology, CRC Press, 2015, 330.

[81] S.Z. Rogovina, E.V. Prut, A.A. Berlin, *Composite materials based on synthetic polymers reinforced with natural fibers*, Polymer Science 61(4 (2019) 417-438.

[82] M. Catauro, S.V. Ciprioti, *Sol-Gel Synthesis and Characterization of Hybrid Materials for Biomedical Applications*, Thermodynamics and Biophysics of Biomedical Nanosystems (2019) 445-475.

[83] M. Faustini, L. Nicole, E. Ruiz-Hitzky, C. Sanchez, *History of Organic-Inorganic Hybrid Materials: Prehistory, Art, Science and*

Advanced Applications, Advanced Functional Materials (2018) DOI: 10.1002/adfm.201704158.

[113] G. Duan, C. Zhang, A. Li, X. Yang, L. Lu, X. Wang, *Preparation and characterization of mesoporous zirconia made by using a poly (methyl methacrylate) template*, Nanoscale Reserch Letter 3 (2008) 118–22.

[115] M. Kasaai, *A review of several reported procedures to determine the degree of N-acetylation for chitin and chitosan using infrared spectroscopy*, Carbohydrate Polymers 71 (2008) 497–509.

[123] ** http://www.spofadental.com/EN/products/dental-resins/denture-base-resins/duracryl-plus/productfamily/DuracrylPlus

[145] D.F.G. Poole, A.W. Brooks, *The arrangement of crystallites in enamel prisms*, Archives of Oral Biology, 5(1) (1961) 14–26;

[150] D.M. Zezell, C. Benetti, M.N. Veloso, P.A.A. Castro, P.A. Ana, Journal of the Brazilian Chemistry Society, 26(12) (2015) 2571-2582;

[158] C. Xu, R. Reed, J. P. Gorski, Y. Wang, M. P. Walker, *The distribution of carbonate in enamel and its correlation with structure and mechanical properties*, Journal of Materials Science, 47(23) (2012) 8035–8043;

[159] V. Dusevich, C. Xu, Y. Wang, M. P. Walker, J. P. Gorski, *Identification of a protein-containing enamel matrix layer which bridges with the dentine–enamel junction of adult human teeth*, Archives of Oral Biology, 57(12) (2012) 1585–1594;

[160] A. Zajac, J. Hanuza, M. Wandas, L. Dyminska, *Determination of N-acetylation degree in chitosan using Raman Spectroscopy*, Spectrochimica Acta A, 134 (2015) 114–120;

[163] B. Kerebel, G. Daculsi, L.M. Kerebel, *Ultrastructural studies of enamel crystallites*, Dental Research, 58 (1979) 844–851;

[164] L. C. Palmer, C. J. Newcomb, S. R. Kaltz, E. D. Spoerke, S. I. Stupp, *Biomimetic systems for hydroxyapatite mineralization inspired by bone and enamel*, Chemical Reviews, 108(11) (2008) 4754–4783;

[165] Q. Ruan, Y. Zhang, X. Yang, S. Nutt, J. Moradian-Oldak, *Amelogenin-chitosan matrix promotes assembly of an enamel-like layer with a dense interface*, Acta Biomaterials, 9(7) (2013) 7289-7297;

[167] Y. Cao, M. L. Mei, Q.-L. Li, E. C. Lo, C. H. Chu, *Enamel prism-like tissue regeneration using enamel matrix derivative*, Journal of Dentistry, 42(12) (2014) 1535-1542;